Proceedings of the 17th World Congress
The International Federation of Automatic Control
Seoul, Korea, July 6-11, 2008

Trajectory Tracking Controller Design for an Unmanned Air Vehicle

Kannan Natesan*. Da-Wei Gu*
Ian Postlethwaite*

**Department of Engineering, University of Leicester, LE2 1HQ UK (Tel: 0044-116-2522567; e-mail: dag@le.ac.uk).*

Abstract: This paper presents a complete trajectory tracking controller design for an Unmanned Air Vehicle using Linear Parameter Varying design methods. The longitudinal and lateral controllers are designed using an inner loop – outer loop structure with the inner loop LPV controller designed using μ-synthesis. The inner-loop is then approximated with a reference model and the outer loop is designed using loop-shaping techniques. Full scale nonlinear simulations are used to test the efficiency of the designed controller and of the proposed design approach.

1. INTRODUCTION

The design of trajectory tracking controllers for autonomous vehicles has been an active area of research in the past few decades. Typically, such controllers use a two loop structure, where the outer loop generates reference signals based on tracking errors and the inner loop uses the reference signals to improve the dynamics (Silvestre *et al*, 2002). As the vehicle dynamics is nonlinear in nature, linear controllers are usually designed at distinct operating points and scheduled through interpolation (Kaminer *et al*, 1998 and references therein) or nonlinear controllers are designed that satisfy design requirements through entire operating region (see for example Aguiar *et al*, 2003 and Frazzoli *et al*, 2000). The main disadvantage of the above methods is that gain-scheduled controllers lack rigorous stability and performance guarantees over the operating region and nonlinear controllers are difficult to implement due to their complex structure. Linear Parameter Varying (LPV) controllers can overcome these drawbacks by systematically incorporating information about variation of vehicle dynamics with scheduling variables.

Over the years several schemes have been employed to achieve closed loop stability and performance for systems that can be expressed in LPV form. Methods that use Linear Matrix Inequalities (LMI) have by far been the most effective in designing LPV controllers. Small-gain theorem is used to exploit the Linear Fractional Transformation (LFT) form of LPV plants to guarantee stability in (Packard, 1994, Apkarian and Gahinet, 1995). Stability and performance is guaranteed in an L_2 sense by using single Lyapunov function in (Packard and Becker, 1992) for all possible plant variations. The technique is extended in (Packard *et al*, 1995) using Bounded Real Lemma formulation for H_∞ performance. The controller is then computed through the solution of a set of LMI. LMIs are reduced to a finite number through the assumption that the plant dynamics depends on the time-varying parameter in an affine fashion. The scheduling variable is also assumed to vary over a convex polytope. Unstructured scaling matrices are used to express existence conditions of LPV controllers through LMIs (Wang and Balakrishnan, 2002). Full-block multipliers are used to express LPV controllers through the solution of a finite number of LMIs in (Wu and Dong, 2006). While the LMI approaches can be effectively used in synthesis of LPV controllers, their main drawback is the computational time required to find a solution. An alternate approach using μ-synthesis is presented in (Shamma and Coutier, 1993) for the design of a missile autopilot using a quasi-LPV approach. The method results in a single controller that exhibits acceptable performance over the entire operating region. A mixed 'LPV-μ' approach is presented in (Biannic *et al*, 1997) to incorporate performance robustness to structured uncertainty in controller design. Though the robustness of the closed loop system to structured uncertainties is enhanced, the synthesis process remains complicated. The LPV controller design methodology presented in this paper exploits the polytopic structure of the inner loop controller to reformulate the gain-scheduling problem into a μ-synthesis problem. The objective of the inner loop is to control an approximated LPV dynamics to match a reference model that remains invariant under different operating conditions. The outer loop is then designed using loop shaping technique which results in a constant controller in this case.

This paper is organised as follows. Section 2 describes the flight control system and explains the controller architecture. Section 3 presents the design of trajectory tracking controller. Section 4 presents full-scale nonlinear simulation results. Finally, Section 5 concludes the paper with main points reemphasised.

2. FLIGHT CONTROL SYSTEM DESCRIPTION AND CONTROLLER CONFIGURATION

2.1 Flight Control System(FCS)

The FCS envisaged for the autonomous Unmanned Air Vehicle (UAV) is shown in Fig. 1. The function of the Mission Management System is the computation of flight path and generation of waypoints and reference signals for autonomous missions. Such waypoints could either be computed from pre-programmed co-ordinated control algorithms or read off from ground to air communication from the Ground Control System through a radio modem. The Guidance and Control block incorporates the control strategy and generates required control signals for the actuators. The Navigation System provides the necessary aircraft navigation states, kinematic parameters and air data for feedback.

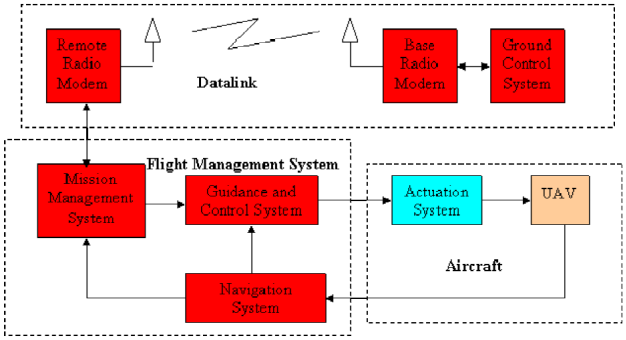

Fig. 1 FCS Architecture

2.2 *Controller Architecture*

The aim of the flight control system is to track waypoints generated by the Mission Management System. The controller architecture for longitudinal and lateral dynamics shown in Fig. 2 and 3 respectively consist of two loops. The inner loop controller is a two-degree-of-freedom LPV controller, designed using μ-synthesis in a model matching approach. The reference model to which the inner loop is matched is then used to design a single outer loop controller. The reference signals for outer loop are height and heading angle for longitudinal dynamics and lateral dynamics, respectively in this study. The outer loop generates reference signals – flight path angle and total velocity for longitudinal mode, and roll angle and side-slip angle for lateral mode – for the inner loops.

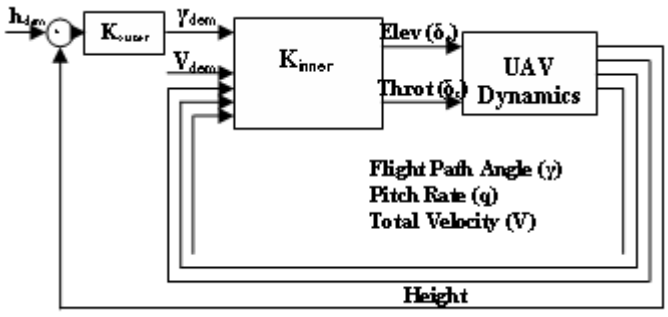

Fig. 2 Longitudinal Controller Architecture

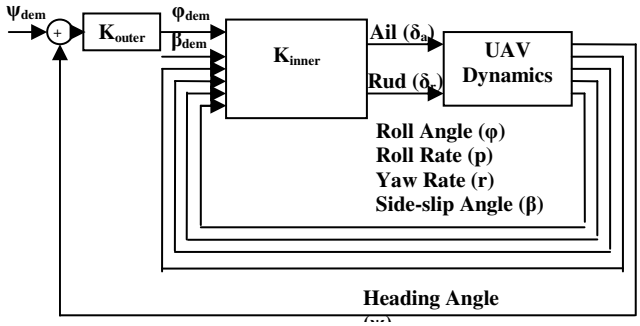

Fig. 3 Lateral Controller Architecture

3. CONTROLLER DESIGN

3.1 *Inner Loop Design*

The autonomous UAV considered in this paper is representative of the class of vehicles that operate at low Reynold's number. Longitudinal and lateral LPV models (Natesan *et al*, 2006) are derived from local linearization of the 6-degree of freedom nonlinear dynamic model and represented as follows:

$$\begin{bmatrix}\dot{u}\\ \dot{w}\\ \dot{\theta}\\ \dot{q}\end{bmatrix} = \begin{bmatrix} X_u(V) & X_w(V) & -g\cos(\theta_1(V)) & X_q(V)\\ Z_u(V) & Z_w(V) & Z_\theta(V) & Z_q(V)\\ 0 & 0 & 0 & 1\\ M_u(V) & M_w(V) & M_\theta(V) & M_q(V)\end{bmatrix}\begin{bmatrix}u\\ w\\ \theta\\ q\end{bmatrix} + \begin{bmatrix} X_{\delta e}(V) & X_{\delta t}(V)\\ Z_{\delta e}(V) & Z_{\delta t}(V)\\ 0 & 0\\ M_{\delta e}(V) & M_{\delta t}(V)\end{bmatrix}\begin{bmatrix}\delta_e\\ \delta_t\end{bmatrix} \tag{1}$$

$$\begin{bmatrix}\dot{v}\\ \dot{p}\\ \dot{r}\\ \dot{\phi}\end{bmatrix} = \begin{bmatrix} y_v(V) & y_p(V) & y_r(V) & y_\phi(V)\\ l_v(V) & l_p(V) & l_r(V) & l_\phi(V)\\ n_v(V) & n_p(V) & n_r(V) & n_\phi(V)\\ 0 & 1 & 0 & 0\end{bmatrix}\begin{bmatrix}v\\ p\\ r\\ \phi\end{bmatrix} + \begin{bmatrix} y_{\delta a}(V) & y_{\delta r}(V)\\ l_{\delta a}(V) & l_{\delta r}(V)\\ n_{\delta a}(V) & n_{\delta r}(V)\\ 0 & 0\end{bmatrix}\begin{bmatrix}\delta_a\\ \delta_r\end{bmatrix} \tag{2}$$

The perturbed states in Eq. (1) for longitudinal dynamics are velocity (u) along the x-axis of the body-axes coordinate system, velocity (w) along the z-axis of the body-axes coordinate system, pitch attitude (θ) and pitch rate (q). δ_e is the elevator input and δ_t is the throttle input. The perturbed states in Eq. (2) for the lateral dynamics are velocity (v) along the y axis, roll rate (p), yaw rate (r) and roll angle(φ). δ_a is the perturbed aileron input and δ_r is the rudder input. The stability and control derivatives in Eqs. (1) and (2) are functions of total velocity and height. However, for UAVs the variation in air density due to change in height is negligible and therefore the only varying parameter is the total velocity V that varies from 22 m/sec to 72 m/sec. The dependence of the dimensional derivatives in Eqs. (1) and (2) on velocity is found by using the method of least-squares curve fit. While the derivatives vary in both linear and quadratic fashions as functions of velocity, only the linear dependence is used to make the problem simple and tractable. The coefficients that most influence the dynamics of the UAV are found by fixing all other coefficients in Eqs. (1) and (2) at their average values, while in turn varying each coefficient over its entire range. It is thus determined that the coefficients X_q, Z_θ, Z_q, M_u, $Z_{\delta e}$ and $M_{\delta e}$ are the most significant derivatives for longitudinal dynamics and Y_p, Y_r, L_v, N_p, N_r, in the sense that any variation in these

coefficients would introduce large changes in the model response for lateral dynamics (See Natesan *et al*, 2006 for more details on LPV modelling).

The closed loop interconnection for longitudinal/lateral inner loop controller design is shown in Fig. 4.

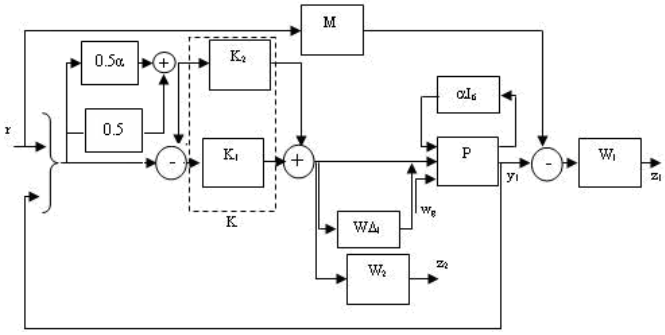

Fig. 4 Interconnection for Inner Loop Control

P is the augmented nominal model obtained for the varying parameter V = 0 in the LPV model in Eqs. (1) and (2). Sensors and actuators are added at the outputs and inputs of the plant in order to make all variations in the plant model occur in the 'A' matrix of the plant P. The state-space realization of P can then be written as:

$$P = \begin{bmatrix} A(V) & B \\ C & 0 \end{bmatrix} \tag{3}$$

In order to formulate the problem in a μ synthesis framework, the uncertainty parameter V is transformed into the uncertainty parameter α satisfying the condition $|\alpha| \le 1$. Since the LPV system considered in this paper is polytopic, the LPV controller can also be chosen as a polytopic controller of the form:

$$K(\theta) = \alpha_1 K_1 + \alpha_2 K_2 \tag{4}$$

where K_1 and K_2 are the controllers designed at the vertices of the velocity polytope, i.e., at 22 and 72 m/sec. α_1 and α_2 are the solutions of the convex decomposition problem:

$$V = \alpha_1 22 + \alpha_2 72$$

Or in the present case, $K(V) = K_1(1-\alpha_2) + \alpha_2 K_2$. Note that the uncertainty parameter α is now given as $\alpha = 2\alpha_2 - 1$. As V varies from 22 to 72 m/sec, α varies from –1 to 1. The feedback system in Fig. 4 can be recast in the form of Fig. 5, where $\Delta = \mathrm{diag}(\alpha I_{11}, \Delta_1)$. Thus, in effect the scheduling parameter α has been 'collected' into the uncertainties that affect the closed loop system and any variation in the plant model also results in variation in the controller. Controller K obtained through μ synthesis yields a single controller K=[K_1 K_2], with the constituent controllers, K_1 and K_2 obtained by making α = -1 and α = 1 respectively.

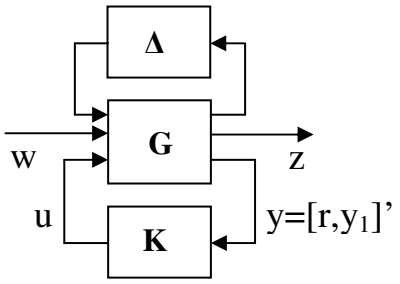

Fig. 5 Representation of the Uncertain Plant under Feedback

The reference model M is chosen to be

$$\frac{100}{s^2 + 20s + 100}\begin{bmatrix} 0 \\ I_{2\times 2} \end{bmatrix}$$

for longitudinal dynamics and lateral dynamics. A damping ratio of 1 and natural frequency of 10 rad/sec are chosen for the matching model from Military Specifications for manned aircraft.

The weighting functions for longitudinal design are selected as:

$$W_1 = \begin{bmatrix} \frac{(100s+1)}{(s^2+20s+1)} & 0 & 0 \\ 0 & \frac{0.0933(s+1000)}{(s+15)} & 0 \\ 0 & 0 & \frac{0.01428(s+1000)}{(s+15)} \end{bmatrix}$$

$$W_2 = \begin{bmatrix} \frac{(0.2s+1)}{(s+80)} & 0 \\ 0 & \frac{(0.2s+1)}{(s+80)} \end{bmatrix}$$

The weighting functions for lateral design are:

$$W_1 = \begin{bmatrix} \frac{(100s+1)}{(s^2+20s+1)} & 0 & 0 & 0 \\ 0 & \frac{(100s+1)}{(s^2+20s+1)} & 0 & 0 \\ 0 & 0 & \frac{0.158(s+1000)}{(s+15)} & 0 \\ 0 & 0 & 0 & \frac{0.38(s+1000)}{(s+15)} \end{bmatrix}$$

$$W_2 = \begin{bmatrix} \frac{(3.2s+28)}{(s+100)} & 0 \\ 0 & \frac{(8s+60)}{(s+100)} \end{bmatrix}$$

The rationale behind the choice of weighting functions can be found in (Natesan *et al*, 2006). Figs. 6 and 7 show the μ bounds for robust performance of the longitudinal and lateral closed loop system. The maximum value of the μ bounds is less than 1, which shows that robust performance is guaranteed for the inner loop. This also means that the inner loop approximates the reference model well. Keeping this in mind, we now design the outer loop controller.

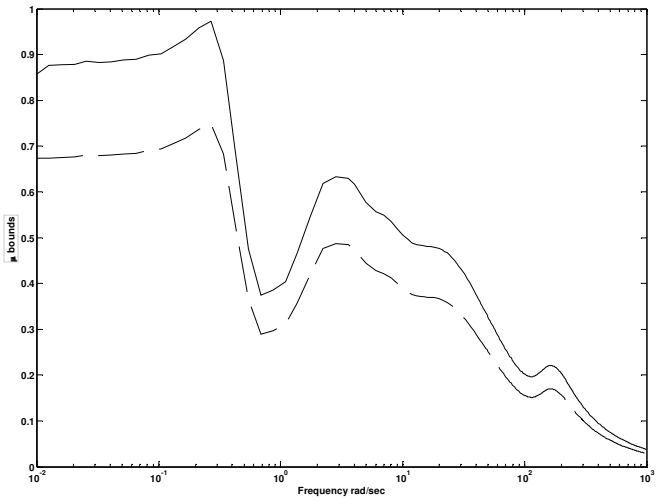

Fig. 6 μ Bounds for Robust Performance – Longitudinal Dynamics

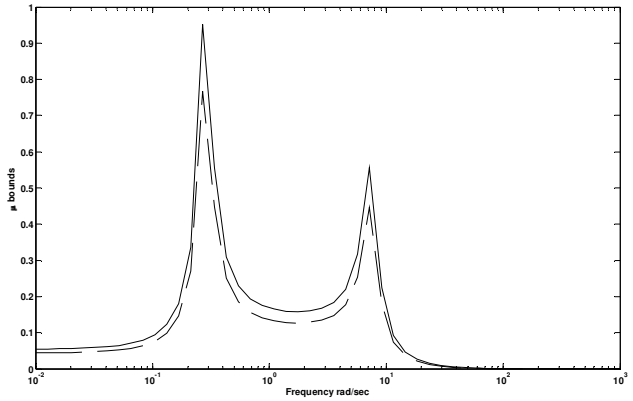

Fig. 7 μ Bounds for Robust Performance – Lateral Dynamics

3.2 Outer Loop Controller

The structure of the outer loop controller is shown in Fig. 8 for both longitudinal and lateral controllers.

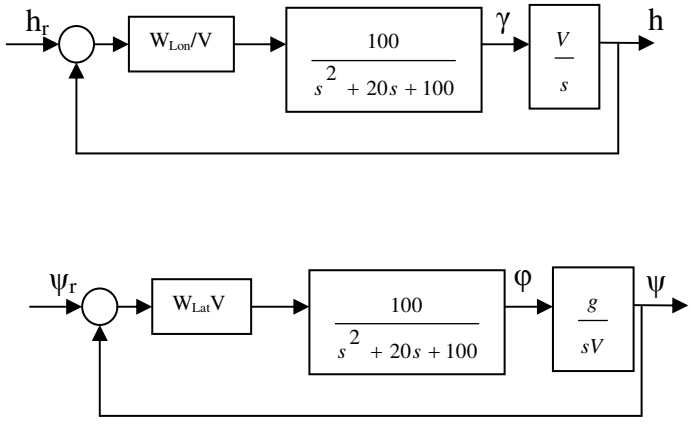

Fig. 8 Closed Loop Interconnection for Outer Loop Controller: Longitudinal (Top) and Lateral Dynamics (Bottom)

The following approximations are used to transform flight path angle γ and roll angle φ into height h and heading angle ψ, respectively:

$$h = \frac{V\gamma}{s}, \quad \psi = \frac{g\varphi}{Vs}$$

The shaped longitudinal and lateral dynamics are now given by $G_{sLon} = \frac{W_{Lon}}{s} G_{lon}$ and $G_{sLat} = \frac{W_{Lat}\, g}{s} G_{lat}$ respectively, where G_{lon} and G_{lat} are the original longitudinal and lateral transfer functions. Total velocity V is used as a multiplicative and divisive factor to make the shaped plant invariant to the scheduling variable. The specifications on the singular values of G_{sLon} and G_{sLat} include high values of $\underline{\sigma}(G_{sLon})$ and $\underline{\sigma}(G_{sLat})$ at low frequencies and low values of $\overline{\sigma}(G_{sLon})$ and $\overline{\sigma}(G_{sLat})$ at high frequencies. A cross-over frequency of 10-20 rad/sec is also chosen for fast closed loop responses. The loop-shaping weights are then given by:

$$W_{Lat} = \frac{0.2s+1}{0.005s+1}, \; W_{Lon} = W_{Lat}/9.81$$

Fig. 8 shows the frequency response of the shaped plant.

The controller is then computed using standard state-space methods (See for example McFarlane and Glover, 1992).

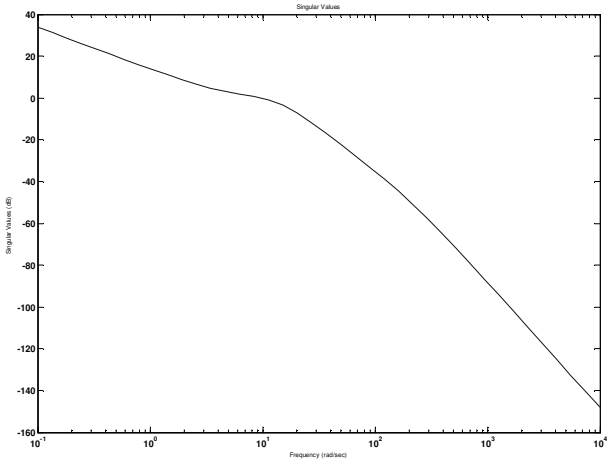

Fig. 8 Frequency Response of the Shaped Plant

4. CLOSED LOOP RESPONSES

In order to test the nonlinear time responses of the closed loop system, full-scale 6DoF simulation is carried out with both inner and outer loop controllers. The aircraft is first trimmed at 1000 m altitude and a ramp signal of 1 m/sec slope is applied to the height reference channel for 30 seconds. The ability of the controller to reschedule itself to varying speed is tested by applying step signals of 5m/sec amplitude in the total velocity channel every 10 seconds. Fig. 9 shows height, total velocity and elevator deflection responses. As can be seen, the UAV tracks the height

reference signal quite well, even in presence of sudden velocity variations. The steady state error of 6% is acceptable considering the fact that the simulation model contains nonlinearities that are not represented in the linear model.

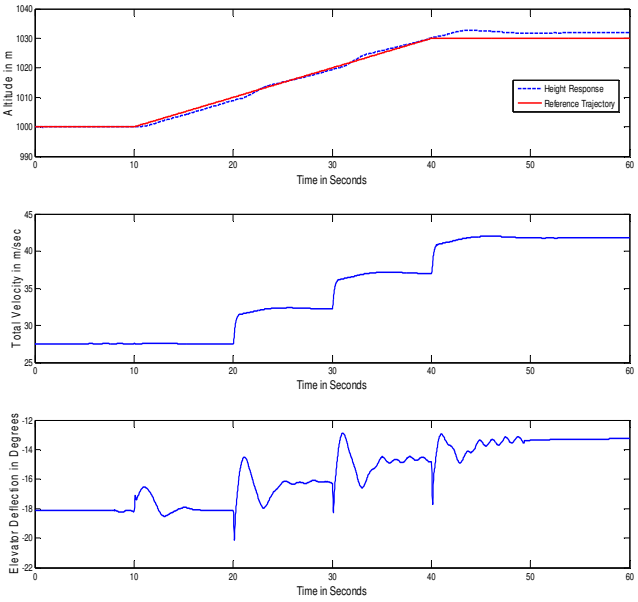

Fig. 9 Nonlinear Simulation Responses to a Ramp Height Reference Signal

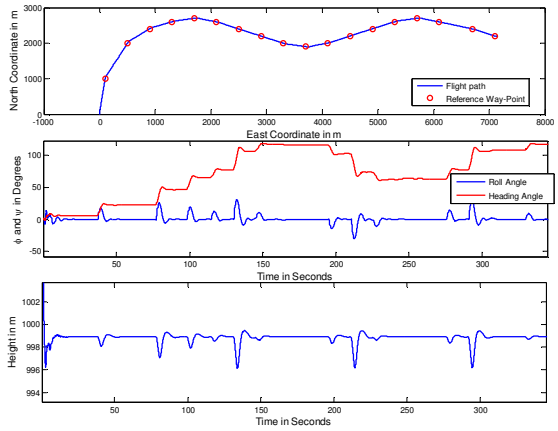

Fig. 10 Nonlinear Simulation Responses to Waypoint Reference Signals

The performance of the lateral controller is tested by applying a set of waypoints in the North-East coordinates to the heading channel. Again the efficiency of the gain-scheduling mechanism is tested by introducing step signals of 5 m/sec amplitude in the velocity channel every 10 seconds. Fig. 10 shows the flight path in the North-East coordinates, roll and heading angles and height responses. As can be seen the UAV maintains a constant altitude of approximately 999 m, with a 1 m error, even in the presence of velocity changes. Such an error in the response is due to improper trimming at the beginning of the simulation. The heading angle and roll angle responses show that the aircraft response is fast with a settling time of 4 seconds.

The simulation results above show that the two-loop control design methodology effectively deals with variations in the scheduling parameter, guaranteeing closed loop stability and performance.

5. CONCLUSIONS

A two-loop trajectory tracking controller is presented in this paper. μ-synthesis is used to design the inner loop gain-scheduled controller while the outer loop controller is designed using loop-shaping approach. Since the inner loop is approximated by a reference model to design the outer loop controller, the design procedure results in simpler implementation. Nonlinear simulations show that the controller effectively tackles variation in scheduling parameter, while tracking the reference trajectory with very little error.

ACKNOWLEDGEMENTS

This research work is supported by the BAE Systems and UK Engineering and Physical Sciences Research Council.

REFERENCES

Aguiar A. P., Cremean L. and Hespanha J. P., Position Tracking for a Nonlinear Underactuated Hovercraft, Controller Design and Experimental Results, In *Proceedings of the 42nd IEEE Conference on Decision and Control*, 2003, pp 3858 – 3863.

Apkarian P., Gahinet P. and Becker G, Self-scheduled H_∞ control of linear parameter-varying systems: a design example, *Automatica*, **Vol. 31**, 1995, pp. 1251 – 1261.

Apkarian P. and Gahinet P., A convex characterisation of gain-scheduling H_∞ controllers, *IEEE Transactions on Automatic Control*, **Vol. 40**, 1995, pp. 853 – 864.

Biannic J. M., Apkarian P. and Garrard W. L., Parameter Varying Control of a High Performance Aircraft, *Journal of Guidance, Control and Dynamics*, **Vol. 20, No. 2**, pp. 225-231, March-April, 1997.

Frazzoli E., Dahleh M. A. and Feron E., Trajectory Tracking Control Design for Autonomous Helicopters using a Backstepping Algorithm, *In Proceedings of American Control Conference*, **Vol. 6**, 2000, pp 4102 – 4107.

Kaminer I., Pascoal A., Hallberg E. and Silvester E., Trajectory Tracking for Autonomous Systems – An Integrated Approach to Guidance and Control, *Journal of Guidance, Control and Dynamics*, **Vol. 21, No. 1**, 1998, pp 29 – 38.

McFarlane D. and Glover K., A Loop Shaping Design Procedure using H_∞ Synthesis, *IEEE Transactions on Automatic Control*, **Vol. 37, No. 6**, 1992, pp 759 – 769.

Natesan K., Gu D-W., Postlethwaite I. and Chen J., Design of Flight Controllers based on Simplified LPV model of a UAV, In Proceedings of IEEE Conference on Decision and Control, **Vol 1,** 2006, pp 37 – 42.

Packard A. and Becker G., Quadratic stabilization of parametrically – dependent linear systems using parametrically-dependent linear, dynamic feedback, *Advances in robust and nonlinear control systems*, 1992, pp. 29-36

Packard A., Gain-scheduling via linear fractional transformations, *System and Control Letters*, **Vol. 22**, 1994, pp. 79 – 92.

Shamma, J. S. and Cloutier, J. R., Gain-scheduled missile autopilot design using linear parameter varying transformations, *Journal of Guidance, Control and Dynamics*, **Vol. 16, No. 2**, 1993, pp 256 – 263.

Silvestre C., Pascoal A. and Kaminer I., On the Design of Trajectory Tracking Controllers, *International Journal of Robust and Nonlinear Control*, **Vol. No. 12**, 2002, pp 797 – 839.

Wang F. and Balakrishnan V., Improved stability analysis and gain-scheduled controller synthesis for parameter-dependent systems, *IEEE Trans on Automatic Control*, **Vol. 47**, 2002, pp 720 – 734.

Wu F. and Dong K., Gain-scheduled control of LFT systems using parameter-dependent Lyapunov functions, *Automatica*, **Vol. 42**, 2006, pp. 39 – 50.